



25 2004). Vision2000, which is an attempt by practicing engineers to improve current codes  
26 in a significant manner, was a pioneering concept in this field. Its aim was to provide PBD  
27 regulations in which performance, hazard levels and acceptance criteria would be  
28 rigorously defined.

29 FEMA273 (FEMA1997) and FEMA356 were developed for the purpose of the  
30 seismic rehabilitation of existing buildings. Four limit states were introduced in FEMA356  
31 (FEMA 2000a) which could be evaluated at different hazard levels by employing linear or  
32 non-linear procedures. These limit states are: Immediate Occupancy (IO), Operational (O),  
33 Life Safety (LS), and Collapse Prevention (CP). FEMA356 later turned into ASCE41-06  
34 (ASCE 2007) and ASCE41-13, which are mandatory regulations in the US. There is a  
35 shortcoming, however, which is that these regulations do not explicitly take into account  
36 either different uncertainties or acceptance criteria which are based on system-oriented  
37 behaviour. In other words, exceeding a limit state in just one structural element is  
38 interpreted as meaning that the whole structure has exceeded the prescribed global  
39 performance level.

40 The various structural limit states have mainly the same definitions in different  
41 regulations. For example, in ASCE41-13, IO corresponds to very minor damage in which  
42 the structural system keeps its stiffness and strength without any residual drift. At the LS  
43 level, moderate damage occurs, but stiffness and strength change slightly. A residual drift  
44 will occur and the structure needs to be repaired. At the CP level, the stiffness and strength  
45 change significantly, although the columns and walls of the building are still able to carry  
46 their gravity loads. Significant residual drift occurs, and the structure will be near collapse.  
47 No further occupancy of the structure is possible.

48 Incremental Dynamic Analysis (IDA) is a method involving comprehensive  
49 nonlinear response history analysis, which has been widely used in the last decade

50 (Vamvatsikos and Cornell 2002). It can be used to define a given structural behaviour from  
51 elastic to extensively inelastic behaviour, by implementing an Engineering Demand  
52 Parameter (EDP) at different Intensity Measure (IM) values. The aleatory uncertainty is  
53 explicitly taken into account in the IDA procedure by including a relatively large set of  
54 ground motion records. Despite the good progress which has already been made, the IDA  
55 calculation method (Vamvatsikos and Cornell 2004 and 2005, Han and Chopra 2006,  
56 Vamvatsikos and Fragiadakis 2010, Dolšek 2009, Asgarian et al 2010, Azarbakht and  
57 Dolšek 2010), the definitions of different limit states on an individual IDA curve still  
58 remain a practical challenge. This issue has different aspects in the case of different  
59 seismic lateral bearing systems. For example, the FEMA350 criteria are based on  
60 experimental data for steel moment frames i.e. Liu and Astaneh-Asl (2000), Lee and  
61 Foutch (2000), Venti and Engelhardt (2000), and Gilton et al (2000). The IO limit state  
62 which corresponds to the Maximum Inter-storey Drift Ratio (MIDR) reaches up to 2 %.  
63 The CP limit state is reached if the MIDR reaches up to 10 %, or if the IDA curve slope  
64 drops to a value which is less than 20 % of the initial (elastic) stiffness. In fact, structural  
65 global behaviour is used to define the limit states in the FEMA350 guideline  
66 (FEMA2000b). On the other hand, on the basis of the ASCE41-13 standard (ASCE/SEI  
67 2014), a set of appropriate plastic hinges needs to be assigned to each element. The  
68 maximum deformation during the response history analysis is then compared to the  
69 acceptable thresholds (provided in the standard). Consequently, when the first element  
70 demand is exceeded, this is taken as the limit state of the structure. In other words, the  
71 ASCE41-13 standard implements an individual-element-oriented criterion in order to  
72 define this limit state.

73         When an element goes beyond the performance threshold, this does not necessarily  
74 mean that the whole structural limit state has been reached. This important issue is

75 addressed in the US Army Corp of Engineers' Manual: Earthquake design and evaluation  
76 of concrete hydraulic structures (USACE 2007), as well as in the FEMAP695 guideline  
77 (FEMA2009). This issue is the main focus of the current study, where it has been assumed  
78 that the seismic design (or assessment) of a specific structure based on the two regulations  
79 should produce nearly the same result. For this reason, two ten-storeyed special steel  
80 moment frame structures were assessed by means of FEMA350, as being representative of  
81 the global behaviour point of view, as well as by ASCE41-13, as being representative of  
82 the element-oriented behaviour point of view. The number of elements, the cumulative  
83 time intervals of demand excess in hinges, the ratio of maximum hinge rotation to capacity  
84 rotation, and the global confidence levels are calculated and discussed in detail in order to  
85 propose a new view-point in this area of research.

86

87

### **Methodology**

88 In order to assess the ASCE41-13 definitions for limit states, two ten-storeyed  
89 special steel moment frame structures were designed based on the ASCE7-10 (ASCE  
90 2010) and AISC (2010) regulations. The first structure was regular in all its aspects,  
91 whereas the second structure was irregular in height. IDA was performed for the given  
92 structures for a set of appropriate ground motion records. The EDP and IM corresponding  
93 to the IO and CP limit states were defined on each IDA curve, based on the FEMA350  
94 guideline. Three new indices were then proposed including: a Cumulative Time Demand  
95 Excess Ratio (CTDER), a Maximum Hinge Demand Excess Ratio (MHDER), and a Ratio  
96 of Demand Excess Elements (RDEE). The CTDER index is expressed mathematically in  
97 Equation (1). This index is calculated for each hinge of a given element and for a given  
98 ground motion. The total damage in each element will clearly increase as the CTDER  
99 index increases.

$$CTDER_{i,k}^j = \left( \frac{t_{ce,i}}{t_{d,k}} \right)_j \quad (1)$$

100 where  $i$  is the element number,  $j$  is the number of the nonlinear behaviour,  $k$  is the record  
 101 number,  $t_{ce,i}$  is the cumulative time for which the demand exceeds the acceptance level  
 102 (based on ASCE41-13), and  $t_{d,k}$  is the total ground motion significant duration (Trifunac  
 103 and Brady 1975).

104 The MHDER index is defined in Equation (2). It shows the magnitude of the demand  
 105 excess in each hinge under the effect of a certain ground motion record. This index, too,  
 106 clearly has a positive correlation with the total damage in each element.

$$MHDER_{i,k}^j = \left( \frac{\theta_{\max,i,k}}{\theta_{\lim}} \right)_j \quad (2)$$

107 where  $\theta_{\max,i,k}$  is the maximum hinge rotation in the  $j^{\text{th}}$  nonlinear behaviour in the  $i^{\text{th}}$   
 108 element in the case of the  $k^{\text{th}}$  ground motion record.  $\theta_{\lim}$  is the acceptable hinge rotation  
 109 based on the ASCE41-13 standard.

110 The RDEE index, defined in Equation (3), takes into account the normalized number of  
 111 elements that are beyond the acceptance criteria based on the ASCE41-13 standard.

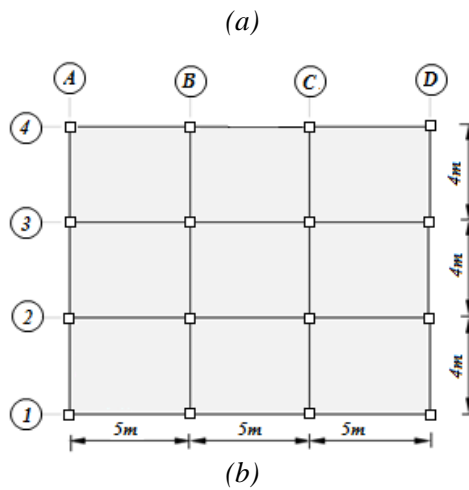
$$RDEE_k^j = \frac{N_{ee,k}^j}{N_{el}} \quad (3)$$

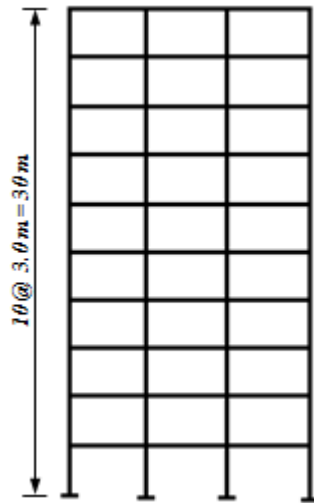
112 It should be mentioned that in this study these indices were calculated for the columns and  
 113 beams separately. The idea was that various combinations of these three proposed indices  
 114 would shed light on the detailed behaviour of the structural system as a whole. This should  
 115 make possible decisions about whether or not the design of a given structure as a whole is  
 116 acceptable. This issue is discussed in detail in the following sections.

117  
118  
119  
120  
121  
122  
123  
124  
125  
126  
127  
128  
129  
130

### Structural Models and Analyses

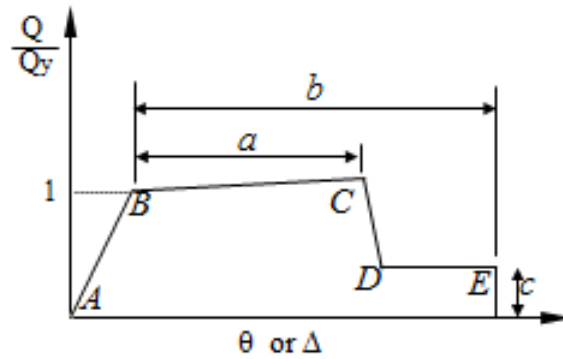
The two investigated ten-storeyed special steel moment frames were designed based on the provisions of AISC 2010, and are shown in Figure 1. The first structure has no irregularities, whereas the second structure has a severe lateral stiffness irregularity in height. Both structures were designed for a highly seismic region, i.e. the Tehran metropolis, and soil type C (based on the ASCE7-10 standard). The dead and live loads on the typical floors are, respectively, equal to 600 kg/m<sup>2</sup> and 200 kg/m<sup>2</sup>. Rectangular box shaped and IPE profiles were used for the column and beam sections, respectively. The effective mass and lateral strength were identical for both structures, and their fundamental period was equal to 1.37s.



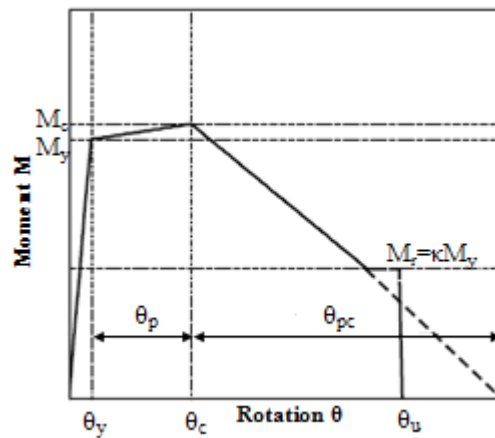


131 Figure 1. Properties of the designed structures in this study, (a) plan view and (b) elevation  
 132 view.

133 The OpenSees platform was utilized in order to perform the nonlinear analyses (*Opensees*).  
 134 In order to simplify the analysis procedure, a 2D model was created. Elastic beam-column  
 135 elements with two nonlinear zero-length elements, at each of the two ends, were used to  
 136 model the beams and columns. The nonlinear backbone curve is defined based on the  
 137 ASCE41-13 standard (ASCE/SEI 2014), and is shown schematically in Figure 2. The  
 138 strain hardening part, marked as the line B-C in Figure 2, has a slope which is equal to 3%  
 139 of the initial (elastic) slope. The Ibarra and Krawinkler model (Ibarra et al. 2005) was  
 140 implemented within the OpenSees platform; it consists of five modelling parameters, as  
 141 can be seen in Figure 3. The five modelling parameters include: (1) the pre-capping plastic  
 142 rotation,  $\theta_p$  (2) the post-capping (i.e. from maximum moment to fracture) plastic rotation,  
 143  $\theta_{pc}$  (3) the cumulative rotation capacity that determines the reference energy dissipation  
 144 capacity of a structural component,  $\Lambda$  (4), the effective-to-predicted component yield  
 145 strength,  $M_y / M_{yp}$  and (5) the capping-strength-to-effective-yield-strength ratio,  $M_c / M_y$ .



146  
 147 Figure 2. The schematic nonlinear backbone for beam and column members (ASCE/SEI  
 148 2014).



149  
 150 Figure 3. The Ibarra-Krawinkler backbone deterioration model (Ibarra et al. 2005).

151 Rayleigh damping proportional to mass and stiffness (Chopra 1995) was assumed by  
 152 considering 5% damping for the first and third modes. The floors were assumed to be rigid,  
 153 and the P-Delta effect was taken into consideration (Mazzoni et al. 2007).

154 The Hunt and Fill algorithm (Vamvatsikos and Cornell 2004) is utilized within the IDA  
 155 algorithm in order to quantify the structural limit states in terms of IM and EDP. The  
 156 spectral acceleration at the fundamental period of structure and five percent damping,  
 157  $S_a(T_1, 5\%)$  was taken as the IM measure, and the MIDR was assumed as the EDP. It is  
 158 worth noting that MIDR has a positive correlation with the structure's global instability, as  
 159 well as with the limit states (FEMA2000b). A total of 25 far-field ground motion records  
 160 were used as input for the IDA (ATC-63 2008). The moment magnitude of the given

162 records was between 6.5 and 7.6, and no directivity effect can be observed among them.  
 163 The characteristics of the records are summarized in Table 1.  
 164 **Table 1.** Characteristics of the 25 ground motion records for the IDA analysis (ATC-63  
 165 2008).

No.	Event	Station	Magnitude	Distance (km)	PGA (g)	Time duration(sec)
1	Kobe, Japan, 1995	Nishi-Akashi, 090	6.9	25.2	0.5	11.25
2	Kobe, Japan, 1995	Shin-Osaka, 000	6.9	28.5	0.24	10.35
3	Kocaeli, Turkey, 1999	Arcelik, 000	7.5	13.5	0.22	11.06
4	San Fernando, 1971	LA-Hollywood Stor FF, 090	6.6	25.9	0.21	13.17
5	Landers, 1992	Coolwater, LN	7.3	20	0.28	10.58
6	Landers, 1992	Coolwater, TR	7.3	20	0.42	8.24
7	Superstition Hills, 1987	Poe Road (temp), 270	6.5	11.7	0.45	13.71
8	Superstition Hills, 1987	Poe Road (temp), 360	6.5	11.7	0.3	13.66
9	Hector Mine, 1999	Hector, 000	7.1	12	0.27	11.68
10	Manjil, Iran, 1990	Abbar, T	7.4	13	0.5	29.12
11	Chi-Chi, Taiwan, 1999	TCU045, E	7.6	26.8	0.47	11.34
12	Chi-Chi, Taiwan, 1999	TCU045, N	7.6	26.8	0.51	10.82
13	Friuli, Italy, 1976	Tolmezzo, 000	6.5	15.8	0.35	4.25
14	Landers, 1992	Yermo Fire Station, 270	7.3	23.8	0.24	17.6
15	Landers, 1992	Yermo Fire Station, 360	7.3	23.8	0.15	18.88
16	Loma Prieta, 1989	Gilroy Array #3, 000	6.9	12.8	0.56	6.37
17	Northridge, 1994	W Lost Cany, 000	6.7	12.4	0.41	6.29
18	Northridge, 1994	W Lost Cany, 270	6.7	12.4	0.48	5.58
19	San Fernando, 1971	LA—Hollywood Stor FF, 180	6.6	25.9	0.17	13.43
20	Kocaeli, Turkey, 1999	Duzce, 180	7.5	15.4	0.31	11.80
21	Kocaeli, Turkey, 1999	Duzce, 270	7.5	15.4	0.36	10.86
22	Loma Prieta, 1989	Capitola, 000	6.9	35.5	0.53	12.15
23	Loma Prieta, 1989	Capitola, 090	6.9	35.5	0.44	13.16
24	Imperial Valley, 1979	Delta, 262	6.5	22.5	0.24	51.43
25	Imperial Valley, 1979	Delta, 352	6.5	22.5	0.35	50.52

166

167

### Limit states Definitions

168 In this section, the seismic performance is assessed by three algorithms, as follows:

169 (1) The IO and CP limit states are controlled by implementing the FEMA350 and  
 170 ASCE41-13 algorithms, respectively, as being representative of system-oriented  
 171 and element-oriented behaviours.

172 (2) CTDER, MHDER and RDEE indices are employed in order to combine the  
 173 element-oriented and the system-oriented point of views. This should help to  
 174 define the structure's behaviour as a whole.

175 (3) The confidence levels, at the IO and CP limit states, are calculated based on the  
 176 element-oriented and system-oriented point of views.

**Element-oriented and system-oriented limit states**

As all the parameters were identical for the structural analysis, it was anticipated that the limit states would be relatively close, based on the FEMA350 and ASCE41-13 algorithms. The IO and CP limit states on the median IDA curve are shown in Figure 4 in the case of the FEMA350 and ASCE41-13 algorithms. As can be clearly seen from this figure, the two above-mentioned algorithms do not result in nearly the same points for the IO and CP limit states. To further investigate this issue, the differences between the IMs, in the cases of the IO and CP limit states, respectively, versus the ground motion records are shown in Figures 5 and 6, from which it can be seen that these differences are more significant in the case of the IO than in the case of the CP limit state. Although this study was not focussed on irregularity effects, it can also be clearly seen from Figures 5 and 6 that the differences are more significant in the case of the irregular structure when compared with the regular structure. On average, the difference between the IMs corresponding to the element-oriented and system-oriented algorithms, were, respectively, 69 % and 42 %, in the case of the IO and CP limit states. These results primarily show that the element-oriented design algorithm (ASCE41-13) results in a significantly more conservative output when compared to the system-oriented design algorithm (FEMA350). This issue is further elaborated in the following sections.

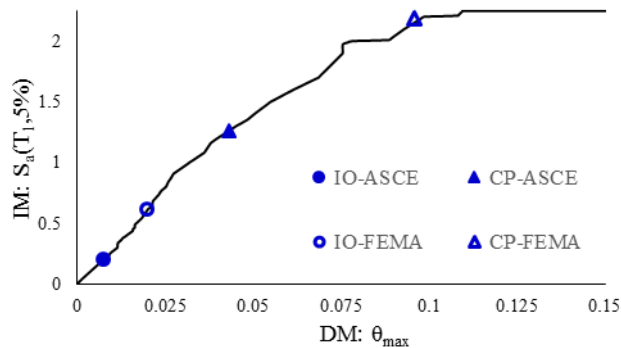
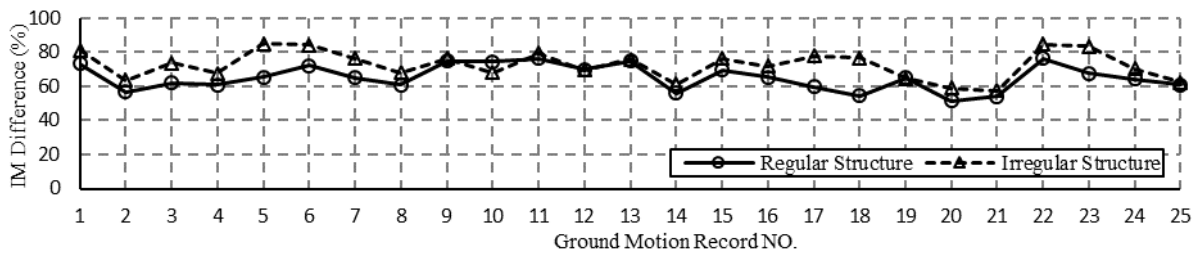
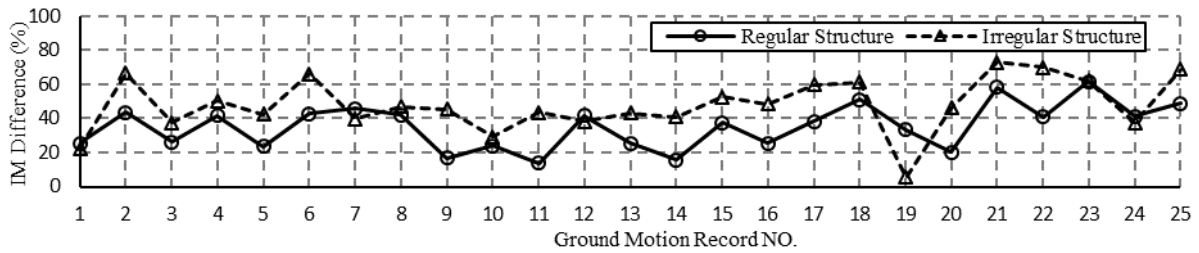


Figure 4. The IO and LS limit states on the median IDA curve of the regular structure obtained on the basis of the FEMA350 and ASCE41-13 regulations.



198  
 199 Figure 5. The difference between the IMs corresponding to the IO limit state versus the  
 200 ground motion records based on the FEMA350 and ASCE41-13 algorithms.



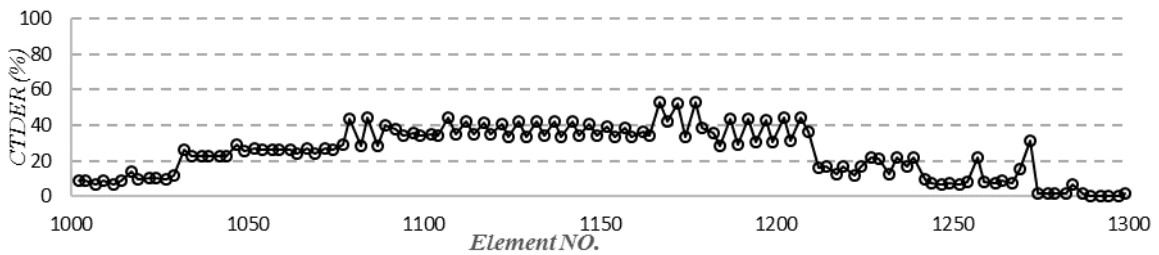
201  
 202 Figure 6. The difference between the IMs corresponding to the CP limit state versus the  
 203 ground motion records based on the FEMA350 and ASCE41-13 algorithms.

204  
 205 **Limit states based on the new proposed indices**

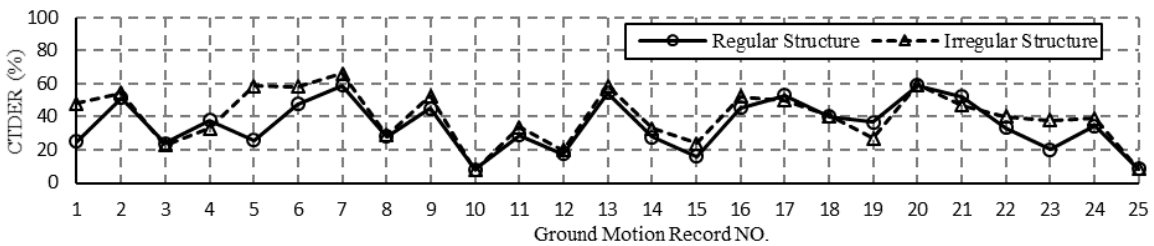
206 In the element-oriented design algorithm, any hinge demand excess corresponds to a  
 207 structural limit state. However, no information about the size of this demand excess is  
 208 available. In other words, the cumulative amount of demand excess in individual hinges  
 209 has to reach to a certain level in order to be able to degrade the total stiffness and strength  
 210 of the structure sufficiently. The IMs corresponding to the IO and CP limit states, based on  
 211 the FEMA350 guidelines, are taken here as benchmarks since the FEMA350  
 212 recommendations are based on extensive experimental data, e.g. see Liu and Astaneh-Asl  
 213 (2000), Lee and Foutch (2000), Venti and Engelhardt (2000) and Gilton et al (2000). The  
 214 CTDER, MHDER and RDEE indices are then calculated independently for the beams and  
 215 columns. For example, the CTDER index shown in Figure 7 corresponds to an IO limit  
 216 state based on the ASCE41-13 standard in the case of the regular structure under the effect

217 of record No. 1. As can be seen in Figure 7, the majority of the beam elements are beyond  
 218 the IO limit state, for at least more than 20 % of the ground motion significant duration.  
 219 The CTDER index is averaged over the whole beam hinges, which presents a 37.5 % data  
 220 point in Figure 8. In fact, Figure 8 shows the average CTDER index versus the different  
 221 ground motion records. As can be seen from this figure, most of the beams show nonlinear  
 222 behaviour beyond the limit state, although this varies between 8 % and 66 %, depending on  
 223 the input ground motion. Figure 9 shows the average MHDER index, only over the  
 224 demand excess elements. This index is up to three and four, respectively, in the cases of  
 225 both the regular and the irregular structure. By averaging over the records, the CTDER  
 226 index is 37.5 % and the MHDER index is 2.87 %.

227 The RDEE index is shown in Figure 10, which confirms that almost 90 % of the beams  
 228 have gone beyond their limit states. On the other hand, no column had any demand excess  
 229 at the IO limit state. A summary of the behaviour of the two investigated structures,  
 230 referring to the IO limit state, is provided in Table 2.

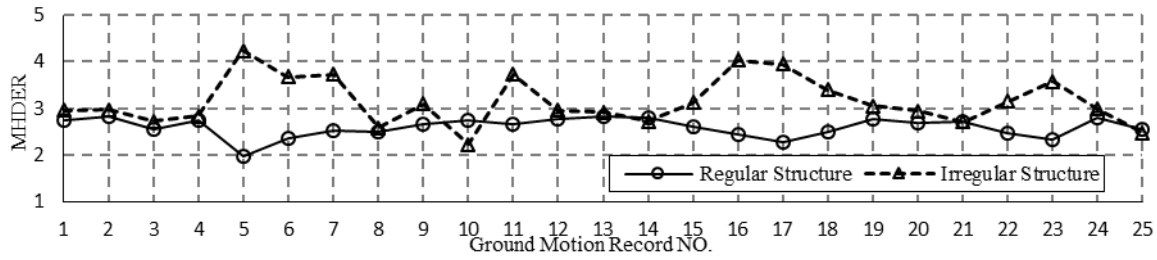


231  
 232 Figure 7. The CTDER index versus different beam elements at an IM corresponding to the  
 233 IO limit state based on ASCE41-13, and the regular structure, under record No.1.

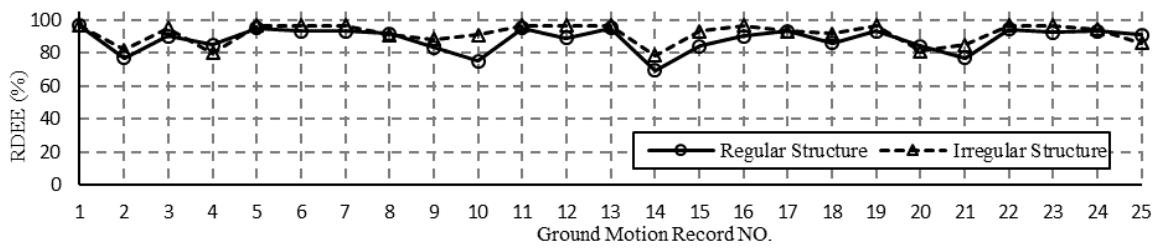


234

235 Figure 8. The beams' average CTDER index versus the different ground motion records in  
 236 the case of the IO limit state based on ASCE41-13.



237  
 238 Figure 9. The beams' average MHDR index versus the different ground motion records in  
 239 the case of the IO limit state based on ASCE41-13.



240  
 241 Figure 10. The beams' RDEE index versus the different ground motion records in the case  
 242 of the IO limit state based on ASCE41-13.

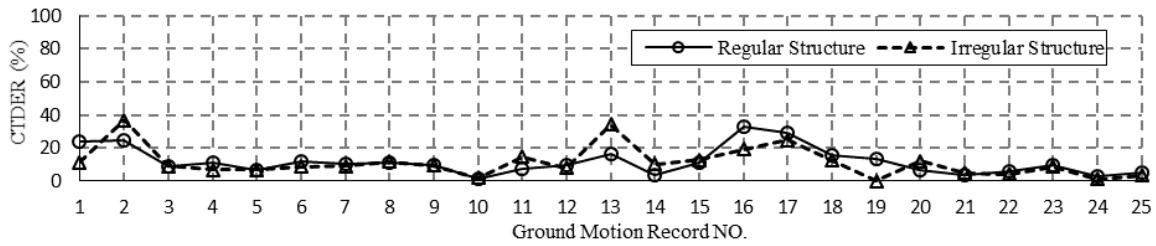
243 **Table 2.** Summary of the proposed indices for the given structures at the IO limit state.

Structural Members	Beams		Columns	
	Regular	Irregular	Regular	Irregular
CTDER	35%	40%	0	0
RDEE	88%	92%	0	0
MHDR	2.6	3.15	0	0

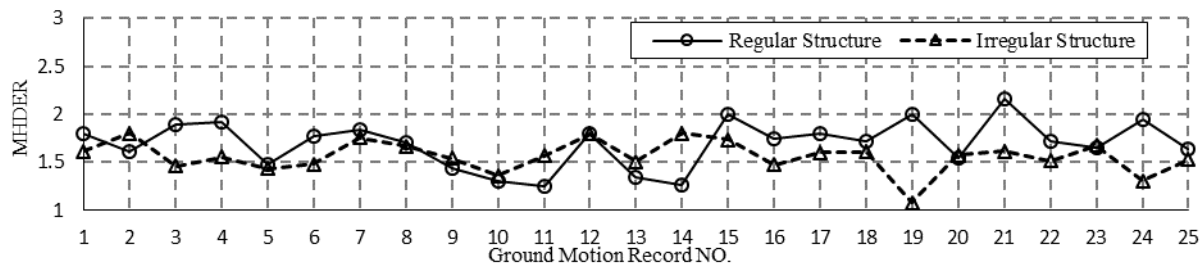
244  
 245 The average values of the CTDER and MHDR indices, and of the RDEE indices for the  
 246 beams, are presented, for the CP limit state, in Figures 11, 12 and 13, respectively. By  
 247 averaging over the records, the CTDER index is 11 %, and the MHDR index is 1.62 %.  
 248 57 % of the beams experience a certain level of demand excess.

249 In the case of the IM corresponding to the CP limit state (based on FEMA350), only the  
 250 demand at the bottom of the first storey columns exceeds the limit state (based on  
 251 ASCE41-13). This behaviour was anticipated, since columns are usually designed more

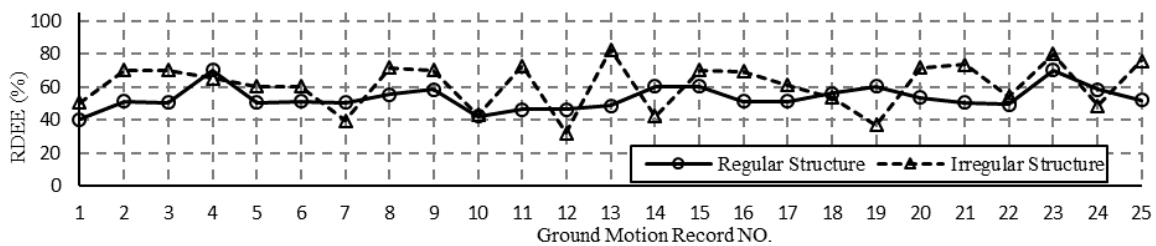
252 conservatively than beams, especially in special moment frames. The average values of the  
 253 CTDER and MHDER indices are shown, respectively, in Figures 14 and 15, in the case of  
 254 the first storey columns. By averaging over the records, the CTDER index is 13.5 %, and  
 255 the MHDER index is 1.66 %. A summary referring to the CP limit state is provided in  
 256 Table 3.



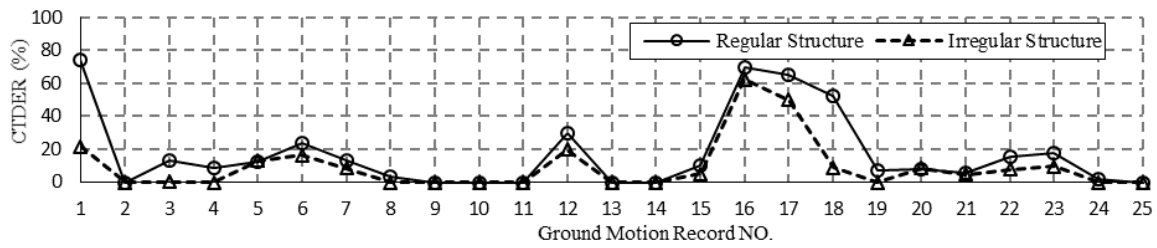
257  
 258 Figure 11. The average CTDER index for the beams versus the different ground motion  
 259 records, in the case of the CP limit state based on ASCE41-13.



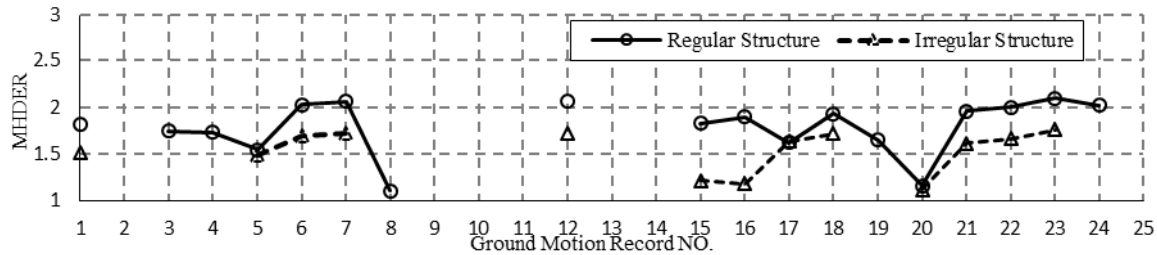
261  
 262 Figure 12. The average MHDER index for the beams, versus the different ground motion  
 263 records, in the case of the CP limit state based on ASCE41-13.



264  
 265 Figure 13. The RDEE index for the beams, versus the different ground motion records, in  
 266 the case of the CP limit state based on ASCE41-13.



267  
 268 Figure 14. The average CTDER index for the first storey columns, versus the different  
 269 ground motion records, in the case of the CP limit state.



270  
 271 Figure 15. The average MHDER index for the first storey columns, versus the different  
 272 ground motion records, in the case of the CP limit state.

273

274 **Table 3.** Summary of the proposed indices for the given structures at the CP limit state.

Structural Members	Beams		Base of Columns	
	Regular	Irregular	Regular	Irregular
CTDER	11%	11%	17%	10%
RDEE	53%	61%	72%	64%
MHDER	1.68	1.56	1.78	1.53

275

276

277 **Confidence levels**

278 The Cornell method (Cornell et al. 2002) is implemented in this section in order to  
 279 calculate the confidence level in each case by taking into account the demand and capacity  
 280 uncertainties. The confidence level is a statistical interpretation of the ratio of the factored  
 281 demand to the factored capacity. One set of factors increases the demand whereas another  
 282 set of factors decreases the capacity in order to account for different uncertainties as well

283 as different regional seismicity characteristics. The seismic demand is calculated by taking  
 284 into account the Tehran metropolis, with  $k=4.07$  and  $b=1.0$ , where  $k$  is the logarithmic  
 285 slope of the hazard curve, and  $b$  is a coefficient which relates the incremental change in  
 286 demand to an incremental change in ground shaking intensity, at the hazard level of  
 287 interest, typically taken as having a value of 1.0 (Cornell et al. 2002). On the other hand,  
 288 the capacity is obtained based on (1) FEMA350 by applying the previously mentioned  
 289 rules on the IDA curves, and (2) ASCE41-13 by monitoring the first hinge which shows a  
 290 demand excess beyond the limit state. A summary of confidence levels for the different  
 291 structures and different algorithms is given in Table 4, from which it can be seen that all  
 292 the confidence levels are above 96 % except in the case of the IO limit state, when using  
 293 the ASCE41-13 regulations. Recalling the Cornell method, the parameter  $\lambda$  is equal to the  
 294 ratio of the factored demand over the factored capacity. Additionally, based on the  
 295 standard Gaussian distribution,  $\lambda=0.86$  is identical to a 90 % confidence level, and higher  
 296 values of the confidence level will be achieved by lower  $\lambda$  values. In other words, as can be  
 297 seen in Table 4, all the  $\lambda$  values are below 0.86 except in the case of the IO limit state when  
 298 using the ASCE41-13 regulations, in which the parameter  $\lambda$  is equal to 1.293 in the case of  
 299 both the regular and the irregular structure. This value of  $\lambda$  results in a 7.9 % confidence  
 300 level, which is not acceptable for design purposes. As these structures were designed based  
 301 on up-to-date design standards, this is proof that the ASCE41-13 standard significantly  
 302 underestimates the capacity corresponding to the IO limit state. Although the capacity  
 303 estimates are quite different in the case of the CP limit state, nevertheless the confidence  
 304 levels are above 96 % in the case of both the FEMA350 and the ASCE41-13 standards.

305 **Table 4.** Confidence levels for the IO and CP limit states, based on the FEMA350 and the  
 306 ASCE41-13 regulations.

Performance Objective	Structure	Capacity Calculation Algorithm	$Sa(T1,5\%)$	$D$	$\gamma$	$\gamma_a$	$C$	$\square$	$\lambda$	$K_x$	$CL$ (%)
-----------------------	-----------	--------------------------------	--------------	-----	----------	------------	-----	-----------	-----------	-------	----------

IO limit state against the 50/50 hazard level	Regular	FEMA350	0.2g	0.0076	1.23	1.035	0.0200	1	0.484	5.15	> 99.7
		ASCE41-13	0.2g	0.0076	1.23	1.035	0.0076	0.9878	1.293	-1.41	7.93
	Irregular	FEMA350	0.2g	0.0063	1.05	1.035	0.0200	1	0.342	7.46	> 99.7
		ASCE41-13	0.2g	0.0063	1.05	1.035	0.0057	0.9329	1.293	-1.41	7.95
CP limit state against the 2/50 hazard level	Regular	FEMA350	0.47g	0.0165	1.17	1.085	0.0895	0.8711	0.268	4.10	> 99.7
		ASCE41-13	0.47g	0.0165	1.17	1.085	0.0432	0.9209	0.525	2.42	99.23
	Irregular	FEMA350	0.47g	0.0141	1.12	1.085	0.0841	0.8222	0.248	4.30	> 99.7
		ASCE41-13	0.47g	0.0141	1.12	1.085	0.0303	0.8288	0.683	1.77	96.15

307 Note: D=median structural demand; C=median structural capacity;  $\gamma$ =demand variability  
308 factor;  $\gamma_a$ = analysis uncertainty factor;  $\phi$ = resistance factor;  $\lambda$ =confidence parameter;  $K_x$ =  
309 standard Gaussian variate associated with the probability x of not being exceeded;  
310 CL=confidence level.  
311

## 312 Conclusions

313 In this study, performance based design was investigated from two different points of  
314 views, as follows: (1) the FEMA350 guidelines, being a representative of system-oriented  
315 behaviour, and (2) the ASCE41-13 standard, being a representative of element-oriented  
316 behaviour. Two regular and irregular structures were assessed by these regulations, and the  
317 Immediate Occupancy and Collapse Prevention limit states were defined. Additionally,  
318 three new indices are proposed in order to justify the differences between the results  
319 obtained by using these two different algorithms. The results show that the element-  
320 oriented algorithm significantly underestimates the seismic capacity in the case of both the  
321 IO and the CP limit states. However, this underestimation results in a reduction of the  
322 confidence level, especially in the case of the IO limit state.

323 At the IO limit state, and based on the FEMA350 regulations, over 90 % of the  
324 beams experience a demand excess beyond the acceptable level. These beams stay, on  
325 average, above the acceptable threshold for 37.5 % of the motion duration. On average, the  
326 plastic rotation in these beams goes up to 280 % beyond the acceptable threshold. On the  
327 other hand, no columns experience any demand excess at this limit state.

328 At the CP limit state, and based on the FEMA350 regulations, over 57 % of the  
329 beams experience a demand excess beyond the acceptable level. These beams stay, on

330 average, above the acceptable threshold for 11 % of the motion duration. On average, the  
331 plastic rotation in these beams goes up to 62 % beyond the acceptable threshold. On the  
332 other hand, at their bases all the first storey columns experience a demand excess in the  
333 case of the majority of the used ground motion records. The demand excess in the first  
334 storey columns, on average in 13 % of the motion duration, reaches up to 66 % beyond the  
335 acceptable level.

336 In summary, the element-oriented algorithm significantly underestimates the seismic  
337 demand when compared to the system-oriented algorithm. It should be mentioned that the  
338 results presented in this paper are limited by the assumptions made, and that further  
339 investigations are necessary to shed more light on this important line of research.

340

341

## References

342 AISC. (2010). "Specification for structural steel buildings." ANSI/AISC 360-10, Chicago.

343 ASCE. (2010). "Minimum design loads for buildings and other structures." ASCE/SEI 7-  
344 10, Reston, VA.

345 ASCE. (2007). "Seismic rehabilitation of existing buildings." ASCE/SEI 41-06, Reston,  
346 VA.

347 ASCE/SEI (Structural Engineering Institute). (2014). "Seismic evaluation and retrofit of  
348 existing buildings." ASCE/SEI 41-13, Reston, VA.

349 Asgarian, B., Sadrinezhad, A., & Alanjari, P. (2010). "Seismic performance evaluation of  
350 steel moment resisting frames through incremental dynamic analysis." *Journal of*  
351 *Constructional Steel Research*, 66(2), 178-190.

352 ATC-63. (2008). Quantification of Building Seismic Performance Factors ATC-63 Project  
353 Report-90% Draft, prepared by the Applied Technology Council for the Federal  
354 Emergency Management Agency.

355 Azarbakht, A. and Dolšek, M. (2011). “Progressive Incremental Dynamic Analysis for  
356 First-Mode Dominated Structures.” *J. Struct. Eng.*, 10.1061/(ASCE)ST.1943-  
357 541X.0000282, 445-455.

358 Bozorgnia, Y., and Bertero, V. V., eds. (2004). *Earthquake Engineering*, CRC Press, New  
359 York.

360 Chopra. A. K. (1995). *Dynamics of structures: theory and applications to earthquake*  
361 *engineering*. Prentice-Hall. Inc., Upper Saddle River, N.J.

362 Cornell, C. A., Jalayer, F., Hamburger, R. O., and Foutch, D. A. (2002). “The probabilistic  
363 basis for the 2000 SAC/FEMA steel moment frame guidelines.” *ASCE J. Struct. Eng.*,  
364 128(4), 526–533.

365 Dolsek, M. (2009). “Incremental dynamic analysis with consideration of modeling  
366 uncertainties.” *Earthq. Eng. Struct. Dyn.*, 38(6), 805-825.

367 FEMA. (1997). “NEHRP guidelines for seismic rehabilitation of buildings.” *Rep. FEMA-*  
368 *273*, FEMA, Washington, DC.

369 FEMA. (2000a). “Prestandard and commentary for the seismic rehabilitation of buildings.”  
370 FEMA-356, Washington, DC.

371 FEMA. (2000b). “Recommended seismic design criteria for new steel moment frame  
372 buildings.” Report No. FEMA-350, SAC Joint Venture, Federal Emergency  
373 Management Agency, Washington, DC.

374 FEMA. (2009). “Quantification of building seismic performance factors.” *Rep. FEMA-*  
375 *P695*, FEMA, Washington, DC.

376 Gilton, C., Chi, B., and Uang, C. M. (2000). “*Cyclic testing of a free flange moment*  
377 *connection.*” *SAC/BD-00/19*, SAC Joint Venture, Sacramento, Calif.

378 Han, W. W., and Chopra, A. K. (2006). "Approximate incremental dynamic analysis using  
379 the modal pushover analysis procedure." *Earthquake Eng. Struct. Dyn.*, 35(15), 1853–  
380 1873.

381 Ibarra, L. F., and Krawinkler, H. (2005). "Global collapse of frame structures under  
382 seismic excitations." Report No. TB 152, The John A. Blume Earthquake Engineering  
383 Center, Stanford Univ., Stanford, CA.

384 Lee, K.-H., Stojadinovic, B. Goel, S. C., Margarian, A. G., Choi, J., Wongkaew, A.,  
385 Reyher, B. P., and Lee, D.-Y. (2000). "Parametric tests on unreinforced connections."  
386 *SAC Background Document SAC/BD-00/01*, SAC Joint Venture, Richmond, Calif.

387 Lee, K., and Foutch, D. A. (2000). "Performance prediction and evaluation of steel special  
388 moment frames for seismic loads." *SAC Background Document SAC/BD-00/25*, SAC  
389 Joint Venture, Richmond, Calif.

390 Liu, J., and Astanek-Asl, A. (2000). "Cyclic tests on simple connections including effects  
391 of the slab." *SAC Background Document SAC/BD-00/03*, SAC Joint Venture,  
392 Richmond, Calif.

393 Mazzoni, S., McKenna, F., Scott, M. H., Fenves, G. L., and Jeremic, B. (2003). *OpenSees*  
394 *command language manual*, Pacific Earthquake Engineering Research Center, Univ.  
395 of California, Berkeley, CA.

396 OpenSees [Computer software]. Berkeley, CA, Univ. of California.

397 Trifunac, M. D., and Brady, A. G. (1975). "A study on the duration of strong earthquake  
398 ground motion." *Bulletin of the Seismological Society of America*, 65(3), 581-626.

399 USACE (U.S. Army Corps of Engineers). (2007). "Earthquake design and evaluation of  
400 concrete hydraulic structures." *Report No. EM 1110-2-6053*, Dept. of the Army,  
401 Washington, DC.

402 Venti, M., and Engelhardt, M. D. (2000). "Test of a free flange connection with a  
403 composite floor slab." *SAC Background Document SAC/BD-00/18*, SAC Joint  
404 Venture, Richmond, Calif.

405 Vamvatsikos, D., and Cornell, C. A. (2002). "Incremental dynamic analysis." *Earthq. Eng.*  
406 *Struct. Dyn.*, 31(3), 491–514.

407 Vamvatsikos, D., and Cornell, C. A. (2004). "Applied incremental dynamic analysis."  
408 *Earthquake Spectra*, 20(2), 523-553.

409 Vamvatsikos, D. and Cornell, C. A. (2005). "Direct estimation of seismic demand and  
410 capacity of multidegree-of-freedom systems through incremental dynamic analysis of  
411 single degree of freedom approximation." *J. Struct. Eng.*, 10.1061/(ASCE)0733-  
412 9445(2005)131:4(589), 589-599.

413 Vamvatsikos, D., and Fragiadakis, M. (2010). "Incremental dynamic analysis for  
414 estimating seismic performance sensitivity and uncertainty." *Earthq. Eng. Struct. Dyn.*,  
415 39(2), 141-163.